Joint kinematics from functional adaptation: A validation on the tibio-talar articulation

Elsevier Editorial System(tm) for Journal of Biomechanics
Manuscript Draft

Manuscript Number: BM-D-15-00119R2

Title: Joint Kinematics from Functional Adaptation: A validation on the Tibio-talar Articulation

Article Type: Full Length Article (max 3500 words)

Keywords: Joint Kinmatics, Subject-specific Modeling, Functional Adaptation, Joint Congruence, Human Ankle

Corresponding Author: Dr. Michele Conconi,

Corresponding Author's Institution: Health Sciences and Technologies - Interdepartmental Center for Industrial Research (HST-ICIR) Alma Mater Studiorum - University of Bologna

First Author: Michele Conconi

Order of Authors: Michele Conconi; Alberto Leardini, Senior Researcher; Vincenzo Parenti-Castelli, Full Professor

Abstract: Biologic tissues respond to the biomechanical conditions to which they are exposed by modifying their architecture. Experimental evidence from the literature suggests that the aim of this process is the mechanical optimization of the tissues (functional adaptation). In particular, this process must produce articular surfaces that, in physiological working conditions, optimize the contact load distribution or, equivalently, maximize the joint congruence. It is thus possible to identify the space of adapted joint configurations (or adapted space of motion) starting solely from knowledge of the shape of the articular surfaces, by determining the envelope of the maximum congruence configurations. The aim of this work was to validate this hypothesis by testing its application on ten human ankle joints. Digitalizations of articular surfaces were acquired in ten in-vitro experimental sessions, together with the natural passive tibio-talar motion, which may be considered as representative of the adapted space of motion. This latter was predicted numerically by optimizing the joint congruence.
The highest mean absolute errors between each component of predicted and experimental motion were 2.07 degrees and 2.29 mm respectively for the three rotations and translations.
The present kinematic model replicated the experimentally observed motion well, providing a reliable subject-specific representation of the joint motion starting solely from articulating surface shapes.

ABSTRACT

Biologic tissues respond to the biomechanical conditions to which they are exposed by modifying their architecture. Experimental evidence from the literature suggests that the aim of this process is the mechanical optimization of the tissues (functional adaptation). In particular, this process must produce articular surfaces that, in physiological working conditions, optimize the contact load distribution or, equivalently, maximize the joint congruence. It is thus possible to identify the space of adapted joint configurations (or adapted space of motion) starting solely from knowledge of the shape of the articular surfaces, by determining the envelope of the maximum congruence configurations. The aim of this work was to validate this hypothesis by testing its application on ten human ankle joints.

Digitalizations of articular surfaces were acquired in ten in-vitro experimental sessions, together with the natural passive tibio-talar motion, which may be considered as representative of the adapted space of motion. This latter was predicted numerically by optimizing the joint congruence.

The highest mean absolute errors between each component of predicted and experimental motion were 2.07 degrees and 2.29 mm respectively for the three rotations and translations.

The present kinematic model replicated the experimentally observed motion well, providing a reliable subject-specific representation of the joint motion starting solely from articulating surface shapes.

INTRODUCTION

The knowledge of the three dimensional joint kinematics is necessary for the understanding of normal and pathological behavior. It provides significant insight into the effects of joint injuries and diseases and allows the design and evaluation of treatments, particularly total joint replacement. A large number of techniques for in-vivo kinematic analysis exist for direct tracking of bone relative motions. Intra-cortical bone-pins (Ramsey and Wretenberg, 1999) provide an accurate though very invasive means of directly measuring skeletal motion under physiological conditions. Stereophotogrammetric fluoroscopy (Fregly et al., 2005) provides acceptable precision but exposes the patient to ionizing radiation and normally reduces the range of joint motion due to the small field of view of the x-ray equipment. Optical tracking of skin mounted markers represents the most non-invasive technique but the relative motion between the skin and the underlying bone, i.e. soft tissue artifacts, makes its accuracy insufficient (Leardini et al., 2005).

A possible alternative to the direct tracking of joint motion is the definition of kinematic models that, based on individual patient anatomy, allow for its indirect estimation. It has been shown how equivalent spatial mechanisms are capable of replicating the same kinematic constraints exerted by ligaments and articular contacts on joint motion both for the knee (Wilson and O'Connor, 1997; Feikes et al., 2003; Ottoboni et al., 2007; Sancisi et al., 2011-b) and the ankle (Franci and Parenti-Castelli, 2009; Franci and Parenti-Castelli, 2008) joints. Unfortunately, the motion calculated by these mechanisms requires both ligament and surface geometries, and is very sensitive to the accuracy with which these anatomical structures are acquired (Sancisi et al., 2011-a). As a result, this approach provides high accuracy when replicating but not forecasting the joint motion.

A different approach, taking into account the behavior of the biological tissues composing the joint, may overcome these limitations. It has been widely documented that connective tissues such as bone, cartilage, tendons and ligaments, possess the capability, often called mechanotransduction, to convert the mechanical strain experienced into biochemical signals (Turner et al., 1995; Burger and Klein-Nulend, 1999; Letechipia et al., 2010; Chen et al., 2000; Ingber, 2008; Kaneko et al., 2009; Grodzinsky et al., 2000; Neu et al., 2007; Leong et al., 2011). These signals participate in governing the action of the cells responsible for the deposition and resorption of the tissues. As a result, tissues are able to modify their structure in response to the mechanical environment to which they are exposed (Robling et al., 2006; Frost, 1990-a; Frost, 1990-b; Burr et al., 1985; Judex et al., 1997; Hsieh and Turner, 2001; Schriefer et al., 2005; Tipton

et al., 1986; Gillard et al., 1979; Frost, 1990-d; Hayashi, 1996; Fujie et al., 2000; Blackwood, 1966; Vogel et al., 1993; Benjamin and Ralphs, 1999; Arokoski et al., 2000; Hudelmaier et al., 2003; Eckstein et al., 2006; Frost, 1990-c; Brommer et al., 2005; Plochocki et al., 2006). This capability was named functional adaptation by Roux (Roux, 1881) and is often also indicated as “Wolff’s law” when considering the bone (Wolff, 1986). Although there is still room for discussion (Bertram and Biewener, 1988; Lanyon, 1987; Lanyon and Rubin, 1984; Lanyon, 1980), functional adaptation seems to produce anatomical structures that use their material optimally, providing the necessary strength with the smallest amount of tissue (Pauwels, 1980; Riggs et al., 1993; Robling et al., 2002).

As an indirect validation of this hypothesis, several biomechanical models are available in the literature, capable of predicting the physiological organization of connective tissues by imposing mechanical optimization with respect to physiological working conditions (Carter, 1987; Huiskes et al., 1987; Smith et al., 1997; Huiskes et al., 2000; Jang and Kim, 2008; van Oers et al., 2008; Vahdati and Rouhi, 2009; Adachiet al., 2010; Giori et al., 1993; Wren et al., 1998; Wren et al., 2000; Carter and Wong, 1988; Heegaard et al., 1999; Carter et al., 2004). Reverting this reasoning and assuming that physiological organization of the tissues is the result of a mechanical optimization, it is possible to identify the physiological working conditions of a joint by searching for the conditions that optimally exploit its architecture. In particular, it has been reported that the correct development (Drachman and Sokoloff, 1966; McMaster and Weinert, 1970; Ruano-Gil et al., 1985; Ward and Pitsillidcs, 1998) and maintenance (Palmoski et al., 1980; Steinberg and Trueta, 1981; Amiel et al., 1982; Paukkonen et al., 1984; Bouvier and Zimny, 1987; Loitz et al., 1989; Smith et al., 1992; Walsh et al., 1993; O'Connor, 1997; Jortikka et al., 1997; Vanwanseele et al., 2002) of the articulating surfaces is modulated by the load and motion experienced at the diarthrodial joint. In other words, functional adaptation must shape the articular surfaces in order to optimize the load transmission throughout the joint motion (Cooney and Chao, 1977; Dekel and Weissman, 1978; Radin et al., 1978; Sokoloff, 1969; Bullough, 1981; Frost, 1999; Heegaard et al., 1999; Hueter, 1862; Volkmann, 1862). As a final consequence, it is theoretically possible to identify the space of motion for which the articular surfaces are adapted (i.e. ‘adapted space of motion’) by searching for the relative position and orientation of the bones in a joint (hereinafter ‘joint configuration’) that maximize the articular capability to distribute an applied load.

The first kinematic model exploiting this concept (Sirkett et al., 2004) tried to reconstruct the carpal bone configuration during the ulnar deviation of the hand, by imposing the maximization of the contact areas during joint motion, evaluated by a proximity criterion (Scherrer et al., 1979; Ateshian et al., 1995; Perie and Hobatho, 1997; Ronsky et al., 1997; Kura et al., 1998; Corazza et al., 2005). However, there was no indication that ulnar deviation is the motion the wrist is optimally adapted for. Further, the amplitude of the contact areas allowed evaluation of the mean contact pressure but not its distribution or peak value and thus was not a good indicator of optimal configurations.

A better evaluation of the capability of a joint in a given configuration to distribute an applied load can be provided by a measure of its congruence. In clinical practice, joint congruence refers to the geometric similarity of two articulating surfaces and it is taken as representative of the joint capability to withstand an applied load under the assumption that the better the two surfaces mate each other, the smaller the peak pressure will be. Thus, a reliable measure of joint congruence may provide a valuable measure of the articular adaptation from a purely geometrical perspective.

In a preliminary work, Conconi and Parenti-Castelli (2012-a) exploited this concept in developing a kinematic model that, requiring solely the knowledge of the articular surfaces shape, forecasted the passive motion of tibio-talar joint by searching for the motion that maximizes the joint congruence, this being evaluated by means of a measure that relies on the Winkler elastic foundation contact model (Conconi and Parenti-Castelli, 2014). The aim of the present paper is to provide an experimental validation of this model by testing its reliability on a number of ankle specimens.

MATERIAL AND METHODS

Analogy between passive and adapted space of motion

When the joint is moving within its adapted space of motion, the ligaments should experience slight length variations. Indeed, while no significant change in ligament length in the joint has been reported as a result of training, experimental evidence shows that ligaments grow in length when

subjected to constant tensioning while they shorten when subjected to a prolonged relaxation (Frost, 1990-4; Fujie et al., 2000; Solomonow, 2009).

Similarly, when cartilage is loaded at physiologic loading frequencies it becomes nearly incompressible and thus should be subject to slight deformation. In fact, dynamic loading extrudes fluid from the superficial layer, consolidating it and decreasing its porosity (Wong and Carter, 2003; Mosher et al., 2005; Setton et al., 1998). This seals the cartilage and blocks further liquid exudation. As a result, cartilage thickness decreases by 5% after a few cycles and then stabilizes, regardless of the performed activity (Eckstein et al., 2006).

As a result, both ligaments and cartilage experience slight deformation when the joint is working within its adapted space of motion. It follows that a motion during which ligaments and cartilage are undeformed should belong to the adapted space of motion. This condition can be found in the passive motion, obtainable in-vitro as a sequence of positions of neutral equilibrium (Wilson and O'Connor, 1997; Wilson et al., 1998). In fact, it has been experimentally shown that ankle ligaments tend to stay isometric during passive motion, particularly the calcaneo-fibular and the tibio-calcaneal ones (Leardini et al., 1999). Also, since no external loads were applied, cartilage deformation can be ignored. Thus, the passive motion can be taken as an idealization of the adapted space of motion.

Experimental Sessions

In the last few years, ten tibio-talar joint specimens were analyzed according to a number of slightly different protocols (Franci et al., 2009, Sancisi et al. 2014). Nevertheless, the recording of the tibio-talar relative motion was performed consistently, making it possible to group and analyze the present ten articulations all together.

The fresh frozen amputated lower limb specimens comprising complete shank and foot, were declared free of anatomical defects by a surgeon, and were fixed through the tibia to a workbench (figure 1.a), leaving the rearfoot free to move, compatibly with the anatomical structures in between. A calcaneal pin protruded from the posterior surface and came into contact with a rigid frame, connected to the workbench by a revolute pair, which supported the pin and drove the tibio-talar joint to move in dorsi/plantar-flexion. Since the weights and the friction between the

pin and the frame were negligible, the overall joint motion was considered as obtained in a virtually unloaded condition. Starting from a rest position in maximum plantarflexion, the joint was extended to maximum dorsiflexion, thus producing the desired complete arc of joint motion, i.e. of the talus with respect to the tibia.

A standard stereophotogrammetric system (Stryker Navigation System; nominal accuracy: ±0.5 degrees, ±0.5 mm) was used for the acquisition of the position of the talus and of the tibia. Two anatomical reference systems were defined, on the tibia (T_f) and the talus (T_c) (Franci et al., 2009) (figure 2), and used for the computation of tibio-talar relative motion, which was expressed by means of a vector $\bar{x}$ of six parameters, three identifying the origin and three defining the orientation by means of a standard sequence-independent Euler angle convention (Grood and Suntay, 1983).

In five cases, after recording of bone motion, it was possible to disarticulate the joint and to digitalize the entire articular surfaces of the talus dome and the distal tibia. In the other five cases (hereinafter denoted with an asterisk), the joint integrity had to be preserved in order make the implant of a prosthesis possible. Thus, in the latter case, the articular surfaces of the top of the talus and the bottom of the tibia could be digitized only partially, by opening the joint capsule and distracting the foot in full plantarflexion.

Each articulating surface was initially represented as a cloud of points in the corresponding anatomical frame and then converted into a triangular mesh model. Where the digitalization was missing or lacking, the articular surface was manually reconstructed from the data of one of the complete specimens.

Measure of joint congruence

From the elastic foundation contact model (Conconi and Parenti-Castelli, 2014), a purely geometrical relation was derived, representing the ratio between the peak pressure p_0 and the amplitude of the pressure distribution resultant force F at the contact. This relation was considered representative of the joint congruence, i.e. the ability of the articulation, in a specific configuration, to distribute an applied load. The derivation of the same relation is here recalled for

189 a generic non-conforming contact (figure 3), but it holds also for highly conforming contacts such
190 as the human ankle articulation here analyzed.

191 Let us consider a rigid body indenting a mattress of springs of constant stiffness k (N/m^3) resting
192 on a rigid base, where no interaction between the adjacent springs is considered (Johnson, 1985).

193 Defining $\delta(x,y)$ as the deformation of the spring at position (x,y), the contact pressure at the
194 same location can be expressed as:

195 $$p(x,y) = k\delta(x,y). \quad (1)$$

196 It follows that the peak pressure p_0 will take place at the position of maximum indentation Δ,
197 namely:

198 $$p_0 = k\delta_{max} = k\Delta. \quad (2)$$

199 Defining A as the projection of the contact surface on a plane orthogonal to z, with dA being the
200 infinitesimal area on which a single spring acts, the resultant F of the pressure distribution can be
201 computed as:

202 $$F = \int_A p(x,y)dA = \int_A k\delta(x,y)dA = k\int_A \delta(x,y)dA = kV, \quad (3)$$

203 where V is the volume of the Boolean intersection of the two undeformed bodies, which
204 corresponds to the dashed area in the cross sectional view of the contact, as depicted in figure 3.

205 Within this contact model, the ratio between the peak pressure and the resultant force becomes
206 purely geometrical, i.e.:

207 $$\frac{F}{p_0} = \frac{kV}{k\Delta} = \frac{V}{\Delta}. \quad (4)$$

208 In practice, joint congruence is evaluated by means of a virtual indentation, achieved by offsetting
209 one bone surface by a prescribed threshold Δ.

210 Let us indicate with S_{tib} and S_{tal} the undeformed and closed surfaces of distal tibia and talus
211 respectively, including both the bone and the articular surface, and with V_{tib} and V_{tal} their volumes

(figure 4). The offset of S_{tib} is indicated with S_Δ, where V_Δ is the volume in it. The volume trapped between S_Δ and S_{tib} is called control volume V_c, i.e.

$$V_c = V_\Delta - V_{tib}. \quad (5)$$

The intersection volume can be measured as the volume of talus within the control volume, i.e.:

$$V = V_c \bigcap V_{tal}. \quad (6)$$

Substituting the real indentation and intersection volume with the virtual ones, the congruence measure CM was obtained from equation 4 as

$$CM = V/\Delta. \quad (7)$$

Clearly, under a prescribed and constant value for the offset threshold Δ, the bigger V is, the more congruent the considered joint will be.

Determination of the adapted space of motion

The general configuration of a joint with N_B bones is described by a vector $\bar{x}$ belonging to a space Σ_G of dimension $6\cdot(N_B-1)$. In fact, once one bone has been chosen as the reference frame, 6 parameters are required to determine the relative position and orientation of each of the other N_B-1 bones.

In general, the adapted space of motion Σ_A is a subset of Σ_G with dimension N. In other words, if the adapted space of motion possesses N DOF, once N parameters of the joint configuration vector $\bar{x}$ are chosen within a physiological range, the remaining $6\cdot(N_B-1)-N$ can be determined by imposing the mechanical optimization, in our case the maximization of joint congruence.

In particular, when considering the tibio-talar joint, N_B is equal to 2 and thus Σ_G corresponds to $\mathbb{R}^6$. Furthermore, the tibio-talar joint may be considered as a single DOF joint (Leardini et al., 1999) and therefore Σ_A is a spatial trajectory in $\mathbb{R}^6$ which can be parameterized, for instance, by

236 the dorsi/plantar-flexion angle. The tibio-talar adapted space of motion can thus be found as the
237 envelope of successive maximum congruence configurations obtained spanning the whole
238 physiological range of ankle flexion.

239 Optimization was performed with Nelder-Mead Simplex algorithm as implemented in the GNU
240 Scientific Library (GSL) while Boolean operations were performed by means of the GNU
241 Triangulated Surface Library (GTS).

242 The objective function was obtained by modifying the congruence measure with the introduction
243 of a penalty term to keep optimization far away from physically impossible configurations where
244 bones penetrate with each other. The final objective function to be maximized became:

245 $$CM = \frac{V_c \cap V_{tal} - k \cdot V_{tib} \cap V_{tal}}{\Delta}. \qquad (8)$$

246 The optimal value for *k* was chosen as the value leading to a residual indentation compatible with
247 human physiology: assuming a mean cartilage thickness of 1.3 mm for each articular surface in the
248 ankle joint (Shepherd and Seedhom, 1999), and admitting deformations of 5% (Eckstein et al.,
249 2006), a 0.13 mm indentation may be considered physiological. A *k* equal to 20 was taken for this
250 aim.

251 With this choice for *k*, the algorithm proved to be almost independent of the choice of Δ (Conconi
252 and Parenti-Castelli, 2012-a; Conconi and Parenti-Castelli, 2012-b), which can thus be chosen
253 arbitrarily. A value of 7 mm was taken in order to maximize the portion of the articular surface
254 within the control volume while preventing other bone features from affecting the congruence
255 measure.

256 The algorithm accuracy was evaluated by means of the mean absolute errors (MAE):
257 corresponding components of the experimental (C_e) and predicted (C_p) joint motion were
258 compared on the whole range of the flexion angle ϕ, with one degree increment. For each
259 component, the norm of differences between C_e and C_p were summed up and divided by the
260 number *n* of the comparisons, i. e.

261 $$MAE = \sum_{i=1}^{n} \frac{\left\| C_e(\varphi_i) - C_p(\varphi_i) \right\|}{n}. \qquad (9)$$

RESULTS

The predicted joint motion from the model compared very well with the corresponding motion from the experimental measurements (figures 5 and 6). The differences between computed and experimental motion were greatest near the extremes of dorsi/plantar-flexion.

The maximum MAE was 2.1° for the rotations, and 2.3 mm for the three translations, though these were smaller than 1 mm in most of the specimens (table 1).

DISCUSSION

From the presented comparison of the results from the model and corresponding in-vitro measurements, we can state that tibio-talar kinematic models based on the functional adaptation of the joint tissues provide a good prediction of the passive motion of this joint, both qualitatively and quantitatively. Previous analysis (Conconi and Parenti-Castelli, 2012-b) has shown that the outcome of the model is not affected by the choice of the component of the configuration vector $\bar{x}$ used for the parameterization of the adapted space of motion. Furthermore, for values of the penalty term k above 10, the algorithm converged to the same space of motion independently of the choice of Δ. Also, the algorithm proved to be very robust with respect to variations of the optimization initial guess (Conconi and Parenti-Castelli, 2012-b). However, a systematic analysis of the model sensitivity to the accuracy of articular surface reconstruction has not yet been performed. In the present study, articular surfaces were reconstructed also from incomplete digitalizations. Missing surface areas were integrated manually from other experimental data. This procedure may have introduced some variation on the real shape of articular surfaces, possibly affecting the model outcome. However, there was no correlation between the size of the digitalized surface and MAE. Despite that, the quality of the final matching between experimental motion and model prediction supports the robustness of the method with respect to the present articular surface representation.

It must be cautioned that the proposed method allows the determination only of the adapted space of motion Σ_A, a subset of the possible joint configurations. Despite this limitation, the

290 determination of Σ_A may provide useful information due to its peculiar characteristics. In fact, a
291 joint working in its adapted space remains in a homeostatic condition, thus reducing the metabolic
292 cost associated with further tissue modification. Also, the analogy with the passive motion
293 characterizes the adapted space of motion as a minimum resistance path, since the forces that
294 drive the joint along it do no or the least work to deform the passive structures. Furthermore, it is
295 worth noting that Carter (1987) suggested a correlation between the risk of microdamage
296 occurrence and accumulation and the strain energy density. Thus, the motion along an adapted
297 path should also reduce the risk of tissue fatigue failure. Finally, adapted configurations represent
298 the healthy functional state of a joint and thus their definition makes the recognition of
299 pathological conditions possible by comparison.

300 If further validated in-vivo, the method here presented can also constitute the initial step for the
301 definition of a fully subject-specific dynamic model of the joint based solely on anatomical
302 measurements. As discussed above, it is in fact possible to kinematically model the human joints
303 by means of mechanisms capable of replicating, between the moving bodies, the same constraints
304 that the joint passive structures exert on the bones they connect. The main advantage of
305 representing the joint by means of an equivalent mechanism is that the kinematic model obtained
306 is built on the subject-specific anatomy and it can be easily generalized into kinetostatic or
307 dynamic models with a sequential approach (Sancisi and Parenti-Castelli, 2011). However, the
308 definition of these mechanisms requires the knowledge of the joint motion. The method here
309 presented allows the determination of such a motion starting solely from a tridimensional
310 representation of the articular surfaces, which may be collected in-vivo, for instance through MRI,
311 and it can thus be considered as the initial step of the sequential approach.

312

313 **CONCLUSION**

314 A non invasive, subject-specific approach for modeling the adapted space of motion of the tibio-
315 talar joint was tested on ten ankle specimens. The present analysis shows good quantitative
316 agreement between the model outcome and the corresponding experimental data, supporting the
317 validity of the method. The kinematic model here obtained allows in particular the evaluation of
318 the adapted space of motion that, due to its characteristics, can be considered as representative
319 of the healthy functioning of the joint. The present determination of a physiological joint motion,

here based on in-vitro digitalization of the articular surfaces, opens the way to the definition of subject-specific joint models built in-vivo from standard medical images, for more personalized treatments and devices.

REFERENCES

Adachi T., Kameo Y. and Hojo M. Trabecular bone remodelling simulation considering osteocytic response to fluid-induced shear stress. *Philos Transact A Math Phys Eng Sci* 2010; 368: 2669-2682.

Amiel D., Woo S. L. et al. The effect of immobilization on collagen turnover in connective tissue: a biochemical-biomechanical correlation. *Acta Orthop Scand* 1982; 53: 325-332.

Arokoski J., Jurvelin J. et al. Softening of the lateral condyle articular cartilage in the canine knee joint after long distance (up to 40 km/day) running training lasting one year. *Int J Sports Med* 1994; 15: 254-260.

Ateshian G. A., Ark J. W. et al. Contact areas in the thumb carpometacarpal joint. *J. Orthop. Res.* 1995; 13: 450-458.

Ateshian G., Rosenwasser M. and Mow V. Curvature characteristics and congruence of the thumb carpometacarpal joint: differences between female and male joints. *J Biomech* 1992; 25: 591-607.

Benjamin M. and Ralphs J. R. Fibrocartilage in tendons and ligaments-an adaptation to compressive load. *J. Anat.* 1998; 193 (Pt 4): 481-494.

Bertram J. E. and Biewener A. A. Bone curvature: sacrificing strength for load predictability? *J. Theor. Biol.* 1988; 131: 75-92.

Blackwood H. J. J. Cellular remodeling in articular tissue. *Journal of dental research* 1966; 43: 480-489.

Bouvier M. and Zimny M. L. Effects of mechanical loading on surface morphology of the condylar cartilage of the mandible in rats. *Acta Anat (Basel)* 1987; 129: 293–300.

Brommer H., Brama P. A. et al. Functional adaptation of articular cartilage from birth to maturity under the influence of loading: a biomechanical analysis. *Equine Vet. J.* 2005; 37: 148-154.

Bullough P. G. The geometry of diarthrodial joints, its physiologic maintenance, and the possible significance of age-related changes in geometry-to-load distribution and the development of osteoarthritis. *Clin. Orthop. Relat. Res.* 1981; 156: 61-66.

Burger E. H. and Klein-Nulend J. Mechanotransduction in bone-role of the lacuno-canalicular network. *FASEB J.* 1999; 13 Suppl: S101-112.

348 Burr D. B., Martin R. B. et al. Bone remodeling in response to in vivo fatigue microdamage. *J Biomech* 1985; 18: 189-
349 200.

350 Carter D. R. Mechanical loading history and skeletal biology. *J Biomech* 1987; 20: 1095-1109.

351 Carter D. R., Beaupre G. S. et al. The mechanobiology of articular cartilage development and degeneration. *Clin.*
352 *Orthop. Relat. Res.* 2004; 427 S: 69-77.

353 Carter D. R. and Wong M. The role of mechanical loading histories in the development of diarthrodial joints. *J. Orthop.*
354 *Res.* 1988; 6: 804-816.

355 Chen C. T., McCabe R. P. et al. Transient and cyclic responses of strain-generated potential in rabbit patellar tendon
356 are frequency and pH dependent. *J Biomech Eng* 2000; 122: 465-470.

357 Conconi M. and Parenti-Castelli V. A sound and efficient measure of joint congruence. *Proceedings of the Institution of*
358 *Mechanical Engineers, Part H: Journal of Engineering in Medicine* 2014; 228(9): 935-941

359 Conconi M. and Parenti-Castelli V. Joint kinematics from functional adaptation: An application to the human ankle. In:
360 *Applied Mechanics and Materials*, Clermont-Ferrand, France, 2012-a, pp. 266-275.

361 Conconi M. and Parenti-Castelli V. Sensitivity and Stability Analysis of a Kinematic Model for Human Joints (An
362 Application to Human Ankle). In: *XII International Symposium on 3D Analysis of Human Movement*, Bologna, Italy,
363 2012-b, pp. 1-4.

364 Connolly K., Ronsky J. et al. Analysis techniques for congruence of the patellofemoral joint. *Journal of Biomechanical*
365 *Engineering* 2009; 131: 124503-1-7.

366 Cooney W. P. and Chao E. Y. Biomechanical analysis of static forces in the thumb during hand function. *J Bone Joint*
367 *Surg Am* 1977; 59: 27-36.

368 Corazza F., Stagni R. et al. Articular contact at the tibiotalar joint in passive flexion. *J Biomech* 2005; 38: 1205-1212.

369 Dekel S. and Weissman S. L. Joint changes after overuse and peak overloading of rabbit knees in vivo. *Acta Orthop*
370 *Scand* 1978; 49: 519-528.

371 Drachman D. and Sokoloff L. The role of movement in embryonic joint development. *Dev Biol* 1966; 14: 401-420.

372 Eckstein F., Faber S. et al. Functional adaptation of human joints to mechanical stimuli. *Osteoarthr. Cartil.* 2002; 10:
373 44-50.

374 Eckstein F., Hudelmaier M. and Putz R. The effects of exercise on human articular cartilage. *J. Anat.* 2006; 208: 491-
375 512.

376 Feikes J., O'Connor J. and Zavatsky A. B. A constraint-based approach to modelling the mobility of the human knee

joint. *J Biomech* 2003; 36: 125-129.

Franci R. and Parenti-Castelli V. A one-degree-of-freedom spherical wrist for the modelling of passive motion of the human ankle joint. In: *Proceedings of IAK 2008, Conference on Interdisciplinary Applications of Kinematics*, Lima, Peru, 2008, pp. 1–13.

Franci R., Parenti-Castelli V., Belvedere C. and Leardini A. A new one-DOF fully parallel mechanism for modelling passive motion at the human tibiotalar joint. *J Biomech* 2009, 42(10):1403–1408.

Fregly B. J., Rahman H. A. and Banks S. A. Theoretical accuracy of model-based shape matching for measuring natural knee kinematics with single-plane fluoroscopy. *J Biomech Eng* 2005; 127: 692–699.

Frost H. M. An approach to estimating bone and joint loads and muscle strength in living subjects and skeletal remains. *Am. J. Hum. Biol.* 1999; 11: 437-455.

Frost H. M. Skeletal structural adaptations to mechanical usage (SATMU): 1. Redefining Wolff's law: the bone modeling problem. *Anat. Rec.* 1990-a; 226: 403-413.

Frost H. M. Skeletal structural adaptations to mechanical usage (SATMU): 2. Redefining Wolff's law: the remodeling problem. *Anat. Rec.* 1990-b; 226: 414-422.

Frost H. M. Skeletal structural adaptations to mechanical usage (SATMU): 3. The hyaline cartilage modeling problem. *Anat. Rec.* 1990-c; 226: 423-432.

Frost H. M. Skeletal structural adaptations to mechanical usage (SATMU): 4. Mechanical influences on intact fibrous tissues. *Anat. Rec.* 1990-d; 226: 433-439.

Fujie H., Yamamoto N. et al. Effects of growth on the response of the rabbit patellar tendon to stress shielding: a biomechanical study. *Clin Biomech (Bristol, Avon)* 2000; 15: 370-378.

Gillard G. C., Reilly H. C. et al. The influence of mechanical forces on the glycosaminoglycan content of the rabbit flexor digitorum profundus tendon. *Connect. Tissue Res.* 1979; 7: 37-46.

Giori N. J., Beaupre G. S. and Carter D. R. Cellular shape and pressure may mediate mechanical control of tissue composition in tendons. *J. Orthop. Res.* 1993; 11: 581-591.

Grodzinsky A. J., Levenston M. E. et al. Cartilage tissue remodeling in response to mechanical forces. *Annu Rev Biomed Eng* 2000; 2: 691-713.

Grood E. S. and Suntay W. J. A Joint Coordinate Systenf for the Clinical Description of Three-Dimensional Motions: Application to the Knee. *Journal of Biomechanical Engineering* 1983; 135: 136-144.

Hayashi K. Biomechanical studies of the remodeling of knee joint tendons and ligaments. *J Biomech* 1996; 29: 707-716.

406 Heegaard J. H., Beaupre G. S. and Carter D. R. Mechanically modulated cartilage growth may regulate joint surface
407 morphogenesis. *J. Orthop. Res.* 1999; 17: 509-517.

408 Hsieh Y. F. and Turner C. H. Effects of loading frequency on mechanically induced bone formation. *J. Bone Miner. Res.*
409 2001; 16: 918-924.

410 Hudelmaier M., Glaser C. et al. Correlation of knee-joint cartilage morphology with muscle cross-sectional areas vs.
411 anthropometric variables. *Anat Rec A Discov Mol Cell Evol Biol* 2003; 270: 175-184.

412 Hueter C. Anatomische Studien an den Extremititengclenken Neugeborener und Erwachsener. *Virchows Arch A Pathol*
413 *Anat Histopathol* 1862; 25: 572-599.

414 Huiskes R., Ruimerman R. et al. Effects of mechanical forces on maintenance and adaptation of form in trabecular
415 bone. *Nature* 2000; 405: 704-706.

416 Huiskes R., Weinans H. et al. Adaptive bone-remodeling theory applied to prosthetic-design analysis. *J Biomech* 1987;
417 20: 1135-1150.

418 Ingber D. E. Tensegrity and mechanotransduction. *J Bodyw Mov Ther* 2008; 12: 198-200.

419 Jang I. G. and Kim I. Y. Computational study of Wolff's law with trabecular architecture in the human proximal femur
420 using topology optimization. *J Biomech* 2008; 41: 2353-2361.

421 Jortikka M. O., Inkinen R. I. et al. Immobilisation causes longlasting matrix changes both in the immobilised and
422 contralateral joint cartilage. *Ann. Rheum. Dis.* 1997; 56: 255-261.

423 Judex S., Gross T. S. and Zernicke R. F. Strain gradients correlate with sites of exercise-induced bone-forming surfaces
424 in the adult skeleton. *J. Bone Miner. Res.* 1997; 12: 1737-1745.

425 Jurvelin J., Kiviranta I. et al. Effect of physical exercise on indentation stiffness of articular cartilage in the canine knee.
426 *Int J Sports Med* 1986; 7: 106-110.

427 Kaneko D., Sasazaki Y. et al. Temporal effects of cyclic stretching on distribution and gene expression of integrin and
428 cytoskeleton by ligament fibroblasts in vitro. *Connect. Tissue Res.* 2009; 50: 263-269.

429 Kiviranta I., Tammi M. et al. Moderate running exercise augments glycosaminoglycans and thickness of articular
430 cartilage in the knee joint of young beagle dogs. *J. Orthop. Res.* 1988; 6: 188-195.

431 Kura H., Kitaoka H. B. et al. Measurement of surface contact area of the ankle joint. *Clin Biomech (Bristol, Avon)* 1998;
432 13: 365-370.

433 Lanyon L. E. Functional strain in bone tissue as an objective, and controlling stimulus for adaptive bone remodelling. *J*
434 *Biomech* 1987; 20: 1083-1093.

435 Lanyon L. E. The influence of function on the development of bone curvature. An experimental study on the rat tibia.
436 *Zool., Lond.* 1980; 192: 457-466.

437 Lanyon L. E. and Rubin C. T. Static vs dynamic loads as an influence on bone remodelling. *J Biomech* 1984; 17: 897-905.

438 Leardini, A., Chiari, L., et al. Human movement analysis using stereophotogrammetry. Part 3. Soft tissue artifact
439 assessment and compensation. Gait Posture, 2005, 21: 212-225.

440 Leardini A., O'Connor J. et al. Kinematics of the human ankle complex in passive flexion; a single degree of freedom
441 system. *J Biomech* 1999; 32: 111-18.

442 Leardini A., Stagni R. and O'Connor J. J. Mobility of the subtalar joint in the intact ankle complex. *J Biomech* 2001; 34:
443 805–809

444 Leong D. J., Hardin J. A. et al. Mechanotransduction and cartilage integrity. *Ann. N. Y. Acad. Sci.* 2011; 1240: 32–37

445 Letechipia J. E., Alessi A. et al. Would increased interstitial fluid flow through in situ mechanical stimulation enhance
446 bone remodeling?. *Med. Hypotheses* 2010; 75: 196-198

447 Loitz B. J., Zernicke R. F. et al. Effects of short-term immobilization versus continuous passive motion on the
448 biomechanical and biochemical properties of the rabbit tendon. *Clin. Orthop. Relat. Res.* 1989; 265-271

449 McLaughlin K., Ronsky J. and Frayne R. In vivo assessment of congruence in the patellofemoral joint of
450 healthysubjects. In: *Proceedings of the XXth ISB Congress-ASB 29th Annual Meeting*, 2005

451 McMaster J. H. and Weinert C. R. Effects of mechanical forces on growing cartilage. *Clin. Orthop. Relat. Res.* 1970; 72:
452 308-314

453 Mosher T. J., Smith H. E. et al. Change in knee cartilage T2 at MR imaging after running: a feasibility study. *Radiology*
454 2005; 234: 245-249

455 Neu C. P., Khalafi A. et al. Mechanotransduction of bovine articular cartilage superficial zone protein by transforming
456 growth factor beta signaling. *Arthritis Rheum.* 2007; 56: 3706-3714

457 O'Connor K. M. Unweighting accelerates tidemark advancement in articular cartilage at the knee joint of rats. *J. Bone*
458 *Miner. Res.* 1997; 12: 580-589

459 van Oers R. F., Ruimerman R. et al. A unified theory for osteonal and hemi-osteonal remodeling. *Bone* 2008; 42: 250-
460 259

461 Ottoboni A., Sancisi N. et al. Equivalent spatial mechanisms for modelling passive motion of the human knee. *J*
462 *Biomech* 2007; 40: S144.

463 Palmoski M. J., Colyer R. A. and Brandt K. D. Joint motion in the absence of normal loading does not maintain normal

articular cartilage. *Arthritis Rheum.* 1980; 23: 325-334.

Paukkonen K., Helminen H. J. et al. Quantitative morphological and biochemical investigations on the effects of physical exercise and immobilization on the articular cartilage of young rabbits. *Acta. Biol. Hung.* 1984; 35: 293-304.

Pauwels F. *Biomechanics of the Locomotor Apparatus.* 1980.

Perie D. and Hobatho M. C. In vivo determination of contact areas and pressure of the femorotibial joint using non-linear finite element analysis. *Clin Biomech (Bristol, Avon)* 1998; 13: 394-402.

Plochocki J. H., Riscigno C. J. and Garcia M. Functional adaptation of the femoral head to voluntary exercise. *Anat Rec A Discov Mol Cell Evol Biol* 2006; 288: 776-781.

Radin E. L., Ehrlich M. G. et al. Effect of repetitive impulsive loading on the knee joints of rabbits. *Clin. Orthop. Relat. Res.* 1978; 288-293.

Ramsey D. K. and Wretenberg P. F. Biomechanics of the knee: Methodological considerations in the in vivo kinematic analysis of the tibiofemoral and patellofemoral joint. *Clinical Biomechanics* 1999; 14: 595-611.

Riggs C. M., Lanyon L. E. and Boyde A. Functional associations between collagen fibre orientation and locomotor strain direction in cortical bone of the equine radius. *Anat. Embryol.* 1993; 187: 231-238.

Robling A. G., Castillo A. B. and Turner C. H. Biomechanical and molecular regulation of bone remodeling. *Annu Rev Biomed Eng* 2006; 8: 455-498.

Robling A. G., Hinant F. M. et al. Improved bone structure and strength after long-term mechanical loading is greatest if loading is separated into short bouts. *J. Bone Miner. Res.* 2002; 17: 1545-1554.

Ronsky J., Van den Bogert A. et al. Application of magnetic resonance imaging for non-invasive quantification of joint contact surface areas. In: *Engineering in Medicine and Biology Society, 1995., IEEE 17th Annual Conference*, 1997, pp. 1253-1254 vol.2.

Roux W. *Der Zuchtende Kampf der Teile, oder die "Teilauslese" im Organismus ("Theorie der Funktionellen Anpassung").* 1881.

Ruano-Gil D., Nardi-Vilardaga J. and Teixidor-Johe A. Embryonal hypermobility and articular development. *Acta Anat (Basel)* 1985; 123: 90-92.

Saamanen A. M., Tammi M. et al. Running exercise as a modulatory of proteoglycan matrix in the articular cartilage of young rabbits. *Int J Sports Med* 1988; 9: 127-133.

Sancisi N., Baldisserri B., Parenti-Castelli V., Belvedere C. and Leardini A. One-degree-of-freedom spherical model for the passive motion of the human ankle joint. Med Biol Eng Comput. 2014; 52(4): 363–73.

493 Sancisi N. and Parenti-Castelli V. A sequentially-defined stiffness model of the knee. *Mechanism and Machine Theory*
494 2011; 46: 1920–1928.

495 Sancisi N., Zannoli D. and Parenti Castelli V. A procedure to analyze and compare the sensitivity to geometrical
496 parameter variations of one-dof mechanisms*. Proceedings of the ASME - IDETC/CIE*, 2011-a, pp. 1-9.

497 Sancisi N., Zannoli D. et al. A one degree-of-freedom spherical mechanism model of the human knee joint.
498 *Proceedings of the Institution of Mechanical Engineers, Part H: Journal of Engineering in Medicine* 2011-b; *225: 725–*
499 *735.*

500 Scherrer P. K., Hillberry B. M. and Sickle D. C. V. Determining the In-Vivo Areas of Contact in the Canine Shoulder.
501 *Journal of Biomechanical Engineering* 1979; 101: 271-278.

502 Schriefer J. L., Warden S. J. et al. Cellular accommodation and the response of bone to mechanical loading. *J Biomech*
503 2005; 38: 1838-1845.

504 Setton L. A., Tohyama H. and Mow V. C. Swelling and curling behaviors of articular cartilage. *J Biomech Eng* 1998; 120:
505 355-361.

506 Shepherd D. E. and Seedhom B. B. Thickness of human articular cartilage in joints of the lower limb. *Ann. Rheum. Dis.*
507 1999; 58: 27-34.

508 Sirkett D., Mullineux G. et al. A kinematic model of the wrist based on maximization of joint contact area. *Proceedings*
509 *of the Institution of Mechanical Engineers, Part H: Journal of Engineering in Medicine* 2004; 218: 349-359.

510 Smith R. L., Thomas K. D. et al. Rabbit knee immobilization: bone remodeling precedes cartilage degradation. *J.*
511 *Orthop. Res.* 1992; 10: 88-95.

512 Smith T. S., Martin R. B. et al. Surface remodeling of trabecular bone using a tissue level model. *J. Orthop. Res.* 1997;
513 15: 593-600.

514 Sokoloff L. *The biology of degenerative joint disease.* 1969.

515 Steinberg M. and Trueta J. Effects of activity on bone growth and development in the rat. *Clin Orthop Relat Res* 1981;
516 156: 52–60.

517 Tipton C. M., Vailas A. C. and Matthes R. D. Experimental studies on the influences of physical activity on ligaments,
518 tendons and joints: a brief review. *Acta Med. Scand. Suppl.* 1986; 711: 157-168.

519 Tummala S., Nielsen M. et al. Automatic quantification of tibio-femoral contact area and congruity. *IEEE Trans Med*
520 *Imaging* 2012; 31: 1404-1412.

521 Turner C. H., Owan I. and Takano Y. Mechanotransduction in bone: role of strain rate. *Am. J. Physiol.* 1995; 269: E438-
522 442.

523 Vahdati A. and Rouhi G. A model for mechanical adaptation of trabecular bone incorporating cellular accommodation
524 and effects of microdamage and disuse. *Mechanics Research Communications* 2009; 36: 284-293.

525 Vanwanseele B., Eckstein F. et al. Knee cartilage of spinal cord-injured patients displays progressive thinning in the
526 absence of normal joint loading and movement. *Arthritis Rheum.* 2002; 46: 2073-2078

527 Vogel K. G., Ordog A. et al. Proteoglycans in the compressed region of human tibialis posterior tendon and in
528 ligaments. *J. Orthop. Res.* 1993; 11: 68-77.

529 Volkmann R. Chirurgische Erfahrungen uber Knochenverbiegungen und Knochenwachsthum. *Virchows Arch A Pathol*
530 *Anat Histopathol* 1862; 24: 512-540.

531 Walsh S., Frank C. et al. Knee immobilization inhibits biomechanical maturation of the rabbit medial collateral
532 ligament. *Clin. Orthop. Relat. Res.* 1993; 253-261.

533 Ward A. C. and Pitsillidcs A. Developmental immobilization induces failure of joint cavity formation by a process
534 involving selective local changes in glycosaminoglycan synthesis. *Trans Orthop Res Soc* 1998; 40: 199.

535 Wilson D. and O'Connor J. A three-dimensional geometric model of the knee for the study of joint forces in gait. *Gait &*
536 *Posture* 1997; 5: 108-115.

537 Wilson D. R., Feikes J. D. and O'Connor J. J. Ligaments and articular contact guide passive knee flexion. *J Biomech* 1998;
538 31: 1127-1136.

539 Wolff J. *The Law of Bone Remodelling.* 1986.

540 Wong M. and Carter D. R. Aticular cartilage functional histomorphology and mechanobiology: a research perspective.
541 *Bone* 2003; 33: 1-13.

542 Wren T. A., Beaupre G. S. and Carter D. R. Tendon and ligament adaptation to exercise, immobilization, and
543 remobilization. *J Rehabil Res Dev* 2000; 37: 217-224.

544 Wren T. A., Beaupre G. S. and Carter D. R. A model for loading-dependent growth, development, and adaptation of
545 tendons and ligaments. *J Biomech* 1998; 31: 107-114.

Figure Legends

Figure 1: The workbench used for the passive motion generation (a) and the digitalization of the articular surfaces (b). In the case depicted in (a), the calcanear motion was also tracked, but not utilized in the present study; the motion of the pin driving the tibio-talar motion is also sketched.

Figure 2: Schematization of the anatomical reference systems for tibia (Tt) and talus (Tc) and the corresponding axes of rotations.

Figure 3: Schematization of the Winkler contact model.

Figure 4: Cross sectional (a) and 3D (b) representation of the determination of the intersection volume V (red dashed area in (a) and red volume in (b)).

Figure 5: Computed (-) vs experimental (- -) motion for the first five specimens.

Figure 6: Computed (-) vs experimental (- -) motion for the last five specimens, digitized without disarticulating the tibio-talar joint.

Table 1: Mean absolute error (MAE) on prono-supination (PS), intra-extra rotation (IE), X, Y and Z displacement, between computed and experimental motion for each of the ten considered specimens. Bold red and green denote maximum and minimum MAE, respectively. An asterisk indicate digitization without disarticulation.

Figure 1

Click here to download Figure: Fig1.doc

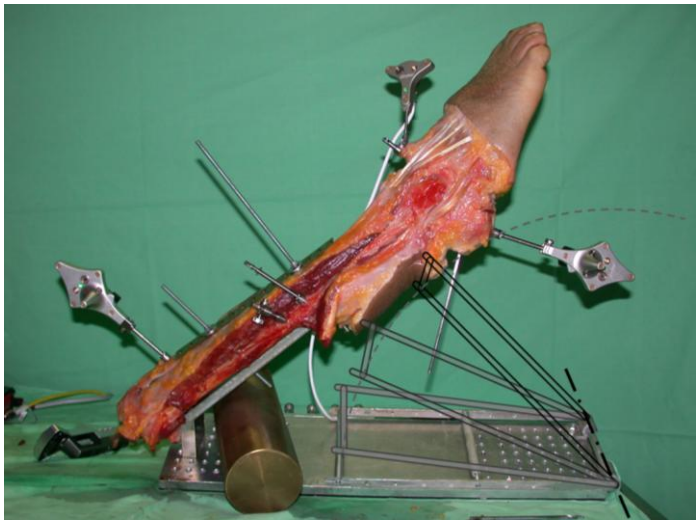

(a)

(b)

Figure 2

Click here to download Figure: Fig2.doc

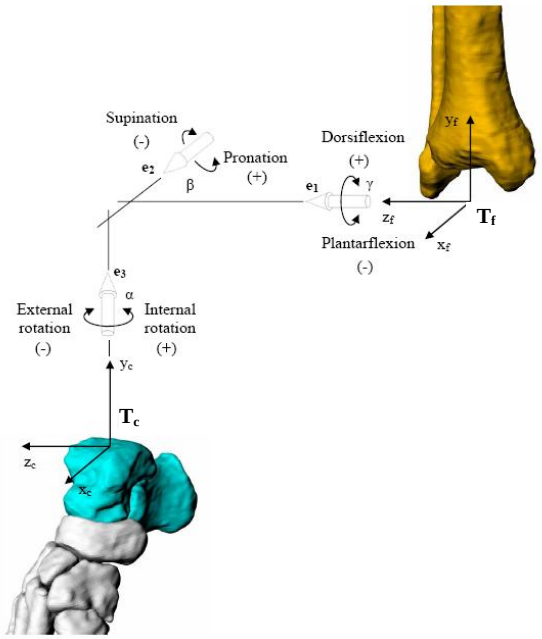

Figure 3

Click here to download Figure: Fig3.doc

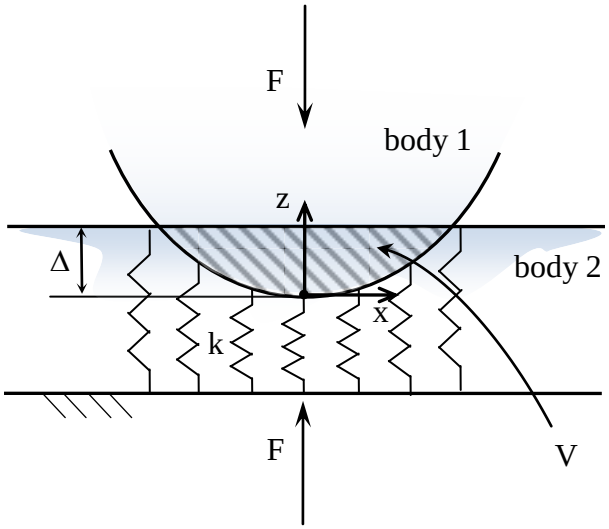

Figure 4

Click here to download Figure: Fig4.doc

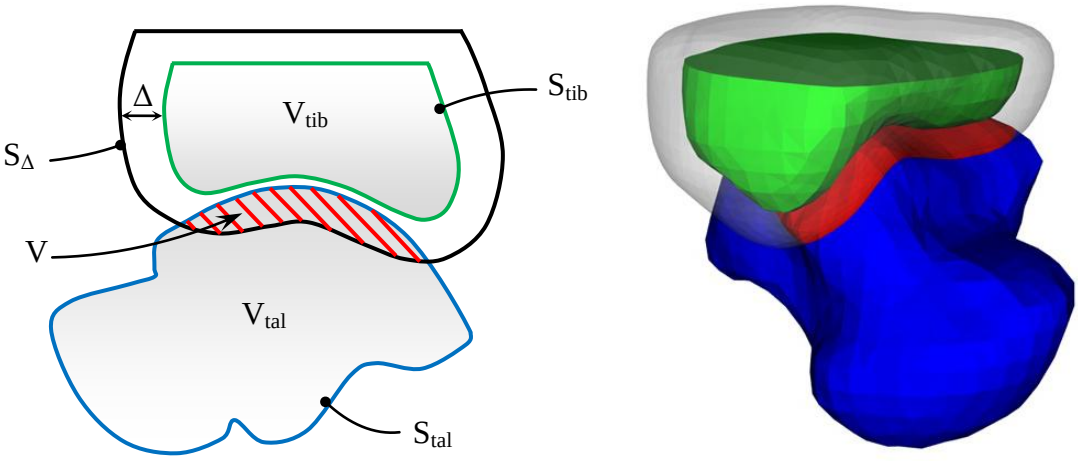

(a) (b)

Figure 5

Click here to download Figure: Fig5.doc

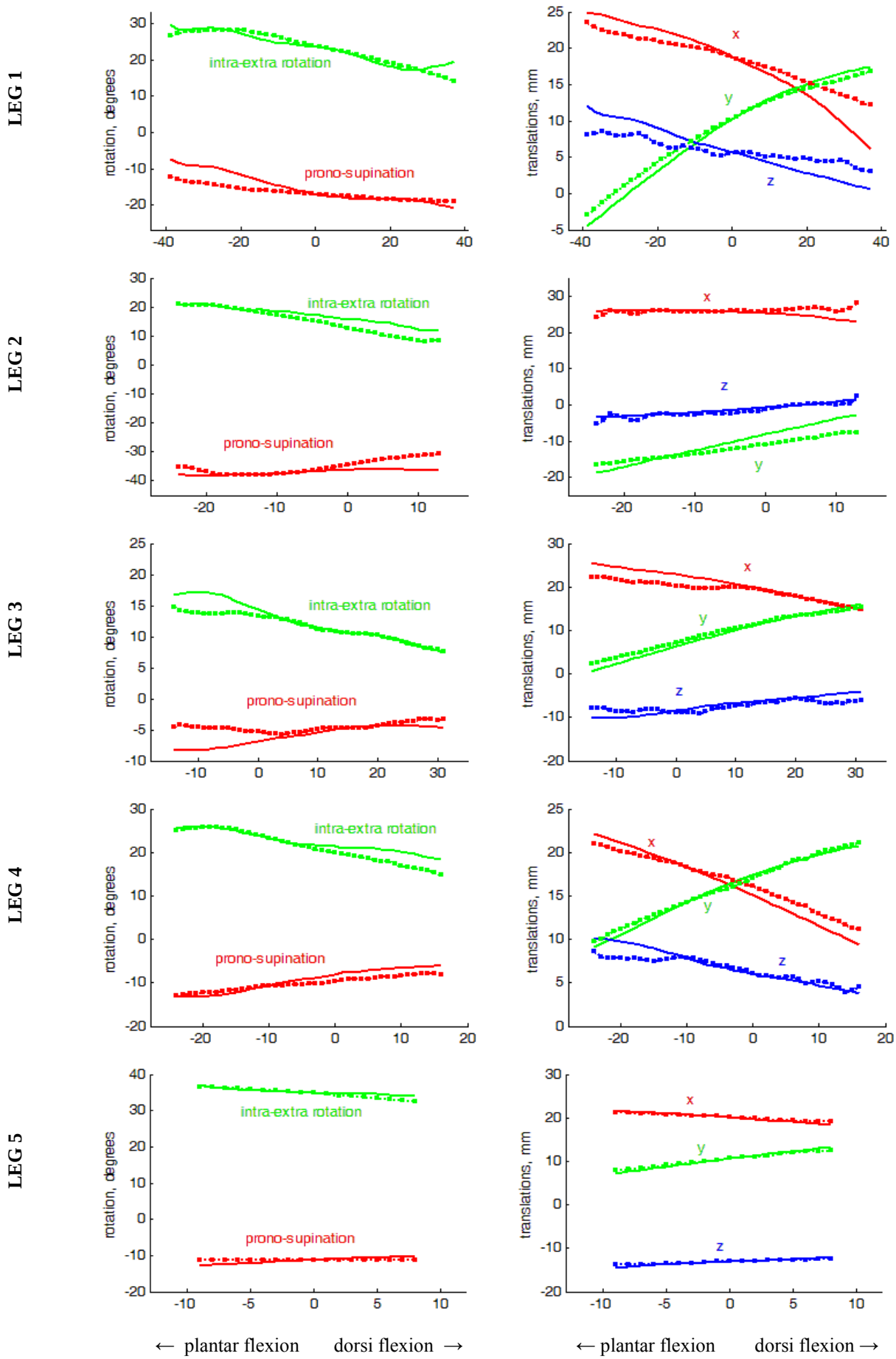

Figure 6

Click here to download Figure: Fig6.doc

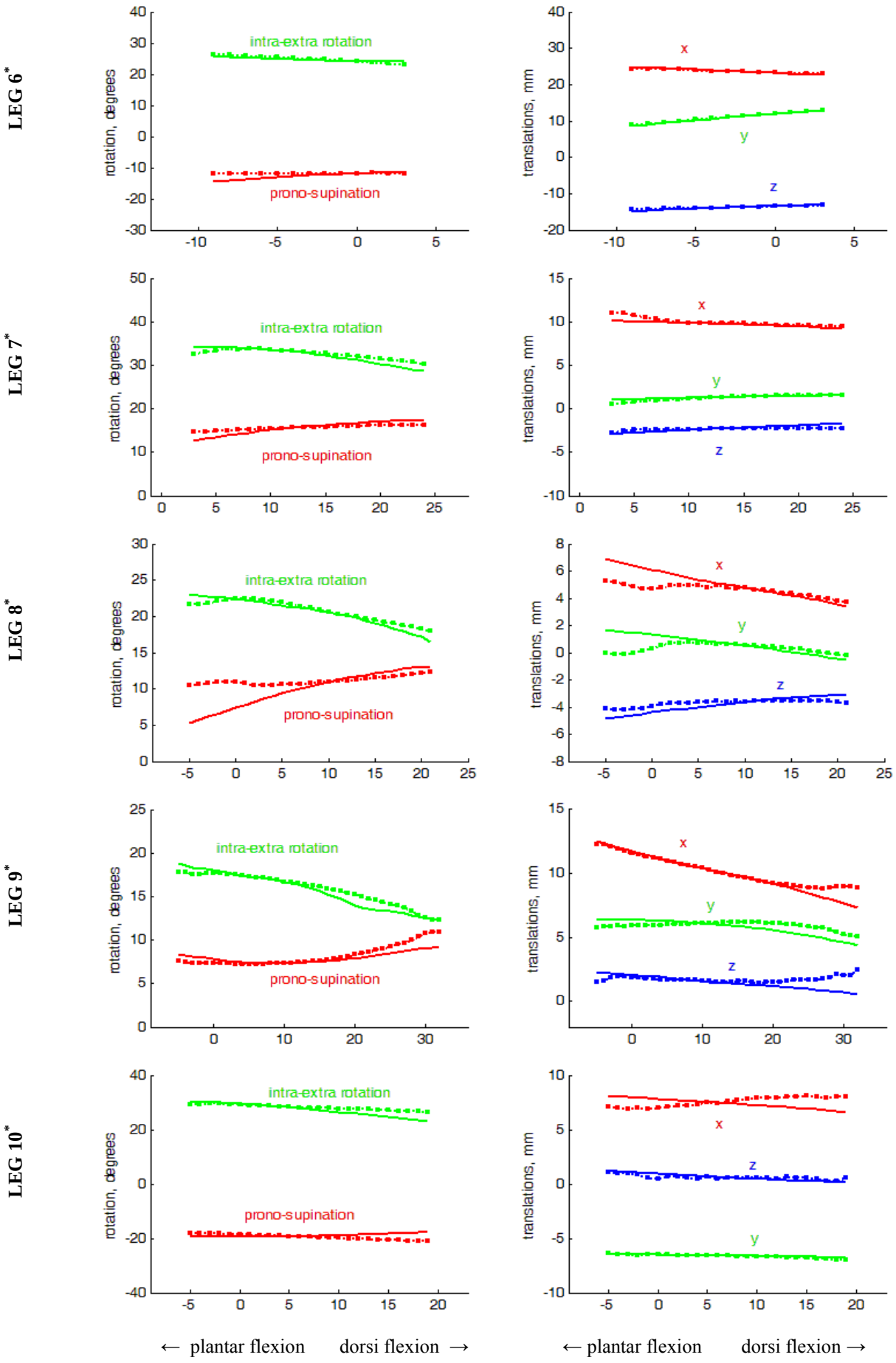

Table

	PS (deg)	IE (deg)	X (mm)	Y (mm)	Z (mm)
LEG 1	1.85	1.03	**1.78**	0.80	**1.75**
LEG 2	**1.89**	**2.07**	1.04	**2.29**	0.59
LEG 3	1.37	0.92	1.41	0.73	1.11
LEG 4	1.15	1.28	0.90	0.31	0.65
LEG 5	0.68	0.49	0.26	0.35	**0.16**
LEG 6*	0.94	**0.42**	**0.18**	0.08	0.18
LEG 7*	0.79	0.72	0.25	0.14	0.22
LEG 8*	1.71	0.51	0.59	0.52	0.35
LEG 9*	**0.53**	0.48	0.29	0.45	0.45
LEG 10*	1.35	1.15	0.76	**0.07**	0.18